

## Time-dependent XAS studies of trapped enzyme-substrate complexes of alcohol dehydrogenase from *Thermoanaerobacter brockii*

Oded Kleifeld, Anatoly Frenkel and Irit Sagi

Copyright © International Union of Crystallography

Author(s) of this paper may load this reprint on their own web site provided that this cover page is retained. Republication of this article or its storage in electronic databases or the like is not permitted without prior permission in writing from the IUCr.

## Time-dependent XAS studies of trapped enzyme-substrate complexes of alcohol dehydrogenase from *Thermoanaerobacter brockii*.

Oded Kleinfeld<sup>a</sup>, Anatoly Frenkel<sup>b</sup>, and Irit Sagi<sup>a\*</sup>

<sup>a</sup>Department of Structural Biology, The Weizmann Institute of Science, Rehovot 76100, Israel. <sup>b</sup>Materials Research Laboratory, University of Illinois at Urbana-Champaign, Urbana, IL 61801, scnyUSAecny  
Email: irit.sagi@weizman.ac.il

The understanding of structure-function relationships in proteins has been significantly advanced with the advent of the biotechnological revolution. A goal yet to be realized for many metalloenzyme systems is to characterize the dynamic changes in structure that bridge the static endpoints provided by crystallography. We present here a series of edge and EXAFS spectra of the metalloenzyme alcohol dehydrogenase from *Thermoanaerobacter brockii* (TbADH) complexed with its substrate. The enzyme-substrate complexes were trapped by fast freezing at various times, following their enzyme activity. Our edge and EXAFS analyses both reveal the time-dependent changes in the structure of the active site of TbADH.

**Keywords:** metalloenzyme, freeze-quench, XAS.

### 1. Introduction.

*Thermoanaerobacter brockii* alcohol dehydrogenase (TbADH) catalyzes the reversible oxidation of secondary alcohols to their corresponding ketones using NADP<sup>+</sup> as the coenzyme (Peretz *et al.*, 1993). Recent crystallographic studies of TbADH have shown that this enzyme is a tetramer comprising four identical subunits (Korkhin *et al.*, 1998). The active site of the enzyme contains a zinc ion that is tetrahedrally coordinated by four protein residues: Cys 37, His 59, Asp 150, and Glu 60. The enzymatic reaction leads to the formation of a ternary enzyme-coenzyme-substrate complex, and catalytic hydride ion transfer is believed to take place between the substrate and coenzyme at the ternary complex (Eklund *et al.*, 1982). Although crystallographic data of various alcohol dehydrogenases and their complexes are available, the mode of action of these enzymes remains to be determined (Eklund *et al.*, 1978, Korkhin *et al.*, 1998). However, it is firmly established that the zinc ion is essential for catalysis. Nevertheless, there is no clear agreement about the coordination environment of the metal ion and the competent reaction intermediates during catalysis.

To determine the mechanism of TbADH, Kleinfeld *et al.* studied the catalytic metal ion environment of the enzyme complexed with the transition state inhibitor dimethyl sulfoxide (DMSO) (Kleinfeld *et al.*, 2000). Interestingly, unlike the mammalian alcohol dehydrogenase (Eklund *et al.*, 1978), TbADH showed a clear expansion in coordination number around the catalytic zinc ion upon binding to DMSO. These results suggested that the central enzyme-substrate complex of TbADH forms a penta-coordination structure at the zinc ion during catalysis.

Yet the exact location of the substrate in TbADH has not been identified by crystallography. Here we show the time-dependent XAS spectra analysis of the ternary complex of TbADH with cofactor NADP<sup>+</sup> and its substrate, 2-butanol. The various ternary complexes of TbADH were trapped at different times by freezing. Our edge and EXAFS data analyses show a significant change in the catalytic zinc ion structure at the various time points of the reaction. These results indicate, for the first time, that the substrate in TbADH is directly bound to the zinc ion during catalysis.

### 2. Materials and Methods.

**Sample preparation** - recombinant TbADH was produced and purified as previously described (Bogin *et al.*, 1997, Peretz *et al.*, 1997). 1 mM TbADH was incubated with 10mM NADP<sup>+</sup> at 4 °C. After a short incubation, 150 mM of 2-butanol was added to the mixture. Aliquots of 30 µL samples were loaded into a sample holder and rapidly quenched by liquid nitrogen. The frozen samples were then mounted into a Displex closed-cycle He cryostat and their temperatures were maintained at 30K.

**Data collection** - XAS data collection was performed at the National Synchrotron Light Source at Brookhaven National Laboratory, beam line X9B. The spectra were recorded at the Zn K-edge in fluorescence geometry at low temperature (30K). The incident beam intensity  $I_0$  was recorded using an ionization chamber, and the fluorescence intensity was recorded using a 13-element Ge detector. The transmission signal from a zinc foil was measured with a reference ion chamber simultaneously with fluorescence for the purpose of the beam energy calibration.

**Data processing and analysis** - The average Zn K-edge absorption coefficient  $\mu(E)$  was obtained after 9-10 independent XAS scans for each sample, which were aligned using the first inflection point of a reference Zn metal foil XAS data (9659 eV). Smooth atomic background was removed using the AUTOBK program of the UWXAFS data analysis package (Stern *et al.*, 1995). Model data for the fitting procedure were constructed by extracting out the catalytic zinc site coordinates (in a radius of 8 Å) from the crystallographic coordinates of TbADH (Korkhin *et al.*, 1998). Using the computer code FEFF7 (Rehr *et al.*, 1991, Zabinsky *et al.*, 1995), we calculated the theoretical photoelectron scattering amplitudes and phase shifts. The theoretical XAFS signal was fitted to the experimental data using the non-linear least squares method implemented in the program FEFFIT (Stern *et al.*, 1995).

### 3. Results and Discussion.

The significance of trapping competent reaction intermediates in alcohol dehydrogenase systems and analyzing them using XAS has been discussed before (Kleinfeld *et al.*, 2000). Most catalytic and biological intermediates possess lifetimes of much less than a second. The rate constant for a single reaction step varies directly in a geometric relationship with the temperature (Stoddard *et al.*, 1996). This means that by lowering the temperature substantially during turnover, it is possible to trap and observe rate-limited reaction intermediates. The advantage for TbADH, being a thermophilic enzyme, is significant for these experiments since lowering the temperature will drastically lower the turnover number and increase the intermediate lifetime. The reaction kinetics of TbADH +NADP<sup>+</sup>+2-butanol was monitored by optical spectroscopy over time. Interestingly, the results show that at the given complex concentration at 8 °C, the enzymatic reaction slows down substantially (the specific activity of the enzyme was

lowered by a factor of 200 relative to its activity at 40°C). Most of the enzymatic catalysis occurs up to 1 minute and reaches equilibrium after 5 minutes (data not shown). The reaction conditions used in this assay are similar to the ones used in our XAS measurements. Figure 1 shows the Zn K-edge spectra of the freeze-quenched complexes of TbADH at various times. Moderate changes in the spectral features of XANES are observed for the different complexes at 9680 eV to 9780 eV. We have therefore assigned these changes to changes in the coordination sphere of the zinc site in TbADH that resulted as the enzymatic reaction progressed.

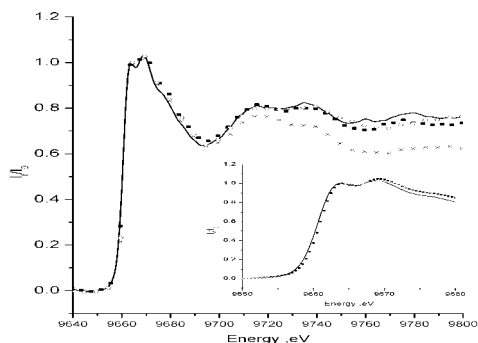


**Figure 1**  
The raw edge spectra of time-dependent XANES data of TbADH+NADP<sup>+</sup>+2-butanol complexes. The samples were freeze-quenched at different time points of the enzymatic reaction as described in the text. 0 min – open circles, 1 min – x, 2 min – filled squares, 5 min – solid line.

The rather small effect on the XANES features can be explained by the existence of a mixture of complexes at each time point. Interestingly, a significant change in edge position (Figure 1 – insert) can be observed among the different complexes, which is consistent with the various edge spectra observed for inhibited TbADH (Kleinfeld *et al.*, 2000). Substantial shifts in energy are directly correlated with changes in the charge distribution around the metal ion, and may also indicate a change in the coordination number (Durham *et al.*, 1988, Kleinfeld *et al.*, 2000, Wirt *et al.*, 1990).

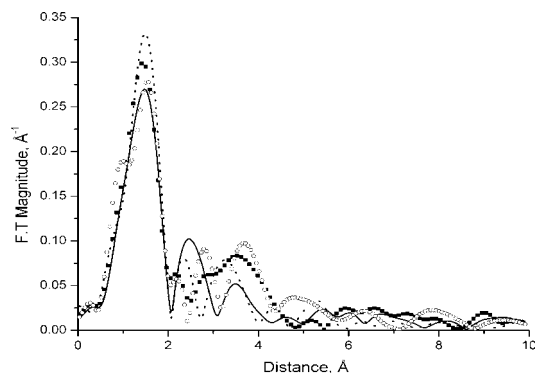


**Figure 2**  
Time-resolved freeze-quench raw EXAFS data of TbADH+NADP<sup>+</sup>+2-butanol complexes at various time points in R-space. 0 min – solid line, 1 min – dashed line, 2 min – filled squares, 5 min – open circles.

The Fourier transforms of the time-resolved EXAFS data are shown in Figure 2. Substantial changes can be observed at the first shell magnitudes and at the shape of the second shell.

Analysis of the EXAFS at the various time points was conducted using the following strategy. The simultaneous curve-fitting mode in FEFFIT was used to fit the various experimental data for all time points concurrently, which allowed to decrease the ratio of the total number of fitting variables to the total number of relevant independent data points. For all complexes, the  $k$  weighting factor was used and the Hanning window function was defined between 2 and 8 Å<sup>-1</sup>. The  $\Delta r$  fitting range was from 1 to 2.1 Å, which corresponded to the first shell.

To reduce the number of fit variables, we fixed the many-body factor  $S_0^2$  at 1.0. The same theoretical paths corresponding to the first shell Zn-N, Zn-O, and Zn-S distances were fit to all data sets simultaneously. The two Zn-O contributions were constrained to be the same, since these bond lengths are proximal to each other in the model.

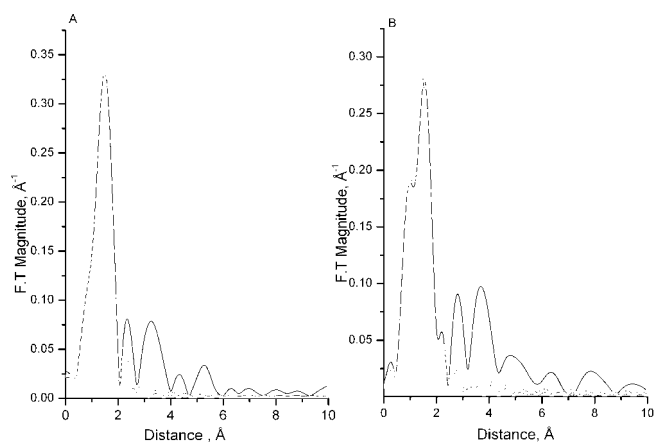


**Figure 3**  
Fourier transform magnitudes of data (solid line) and fit (open circles) corresponding to the second fitting procedure (Table 1) at times of (A) 1 minute and (B) 5 minutes after mixing. The corresponding fit parameters are listed in Table 1.

The representative fits of FEFF theory to the data are shown in Figure 3. The results of the EXAFS data analysis are shown in Table 1. The results shown in Table 1 outline the fitting strategy and the various constraints that were used in the fitting procedure. In the first step, Fit1 (Table 1), the  $\Delta r$  and the Debye-Waller factors  $\sigma^2$  of the Zn-N and Zn-S contributions were constrained to be equal for all data sets. Interestingly, the increase occurred in the Zn-O coordination number and in the bond distances at higher time points. In order to further decrease the number of variables, we performed the second iterative step, Fit 2 (Table 1), where the constrained parameters in Fit 1 were fixed. The results of this fit were consistent with those of Fit 1. The results obtained in Table 1 were not sensitive to the details of this and other iterative fitting approaches tried.

However the improvement of the data analysis strategy is needed in order to prove the uniqueness of our solution. Nevertheless, the combination of the edge spectra and the EXAFS results suggest that the substrate molecule in TbADH is directly bound to the zinc ion during catalysis, which is consistent with the binding of the transition state analogue DMSO to TbADH (Kleinfeld *et al.*, 2000).

| Fit 1 |            |                                |          |           |                                |            |                                |
|-------|------------|--------------------------------|----------|-----------|--------------------------------|------------|--------------------------------|
| Time  | Zn-N       |                                | Zn-O     |           |                                | Zn-S       |                                |
|       | R[Å]       | $\sigma^2$ , [Å <sup>2</sup> ] | N        | R [Å]     | $\sigma^2$ , [Å <sup>2</sup> ] | R [Å]      | $\sigma^2$ , [Å <sup>2</sup> ] |
| 0 min | 1.83[4] V* | 1E-4 V*                        | 1.8[4] V | 1.98[1] V | 3E-3 V                         | 2.21[1] V* | 2E-6 V*                        |
| 1 min | 1.80[4] V* | 1E-4 V*                        | 2.2[4] V | 1.99[1] V | 3E-6 V                         | 2.21[1] V* | 2E-6 V*                        |
| 2 min | 1.83[4] V* | 1E-4 V*                        | 3.3[7]V  | 1.99[1] V | 1E-2 V                         | 2.21[1] V* | 2E-6 V*                        |
| 5 min | 1.83[4] V* | 1E-4 V*                        | 3.9[4] V | 2.07[3] V | 6E-3 V                         | 2.21[1] V* | 2E-6 V*                        |
| Fit 2 |            |                                |          |           |                                |            |                                |
| 0 min | 1.85       | 1E-3                           | 2        | 2.00      | 5E-3                           | 2.2        | 1E-6                           |
| 1 min | 1.85 F     | 1E-3 F                         | 2.2[5] V | 2.00[1] V | 1E-6 V                         | 2.2 F      | 1E-6 F                         |
| 2 min | 1.85 F     | 1E-3 F                         | 3.8[6] V | 2.01[1] V | 1.5E-2 V                       | 2.2 F      | 1E-6 F                         |
| 5 min | 1.85 F     | 1E-3 F                         | 3.7[3] V | 2.08[1] V | 4E-3 V                         | 2.2 F      | 1E-6 F                         |

**Table 1.** Results of simultaneous EXAFS curve-fitting analysis for time dependent complexes of TbADH+NADP<sup>+</sup>+2-butanol. The symbols F,V stand for “fixed” and “varied”, respectively, and indicate how the respective parameter was treated in the fit. \* indicates that the given fitting parameters were constrained to be the same in all data sets. In Fit 2, the time 0 data set was fitted separately and the best fits were used to set R and  $\sigma^2$  of Zn-N and Zn-S paths in the simultaneous fit (1-5 min).

In this work we attempt to analyse time-resolved XAS data of biological system in a quantitative way. At this stage, our results show the feasibility of such experiments and emphasize the need for a combination of various data analysis strategies, such as principal component analysis, in addition to the fitting method described in this work.

This work was supported by the Bi-National Scientific Foundation (grant #6602/2). A.Frenkel acknowledges support from the U.S. DOE Grant No. DEFG02-96ER45439 through the Materials Research Laboratory at the University of Illinois at Urbana-Champaign (AIF) and by the Office of Biological and Environmental Research of the U.S. DOE under Prime Contract No. DE-AC02-98CH10886 through the Brookhaven National Laboratory (MV).

**References**

Bogin, O., Peretz, M. and Burstein, Y. (1997), *Protein Sci*, **6**, pp. 450-458.  
 Durham, P.J., *Theory of XANES*, Wiley-Interscience Publication, Eindhoven, 1988.  
 Eklund, H. and Branden, C. (1978), *J. Biochem. Chem.*, **254**, pp. 3458-3461.  
 Eklund, H., Plapp, B.V., Samama, J.P. and Branden, C.I. (1982), *J. Biol. Chem.*, **257**, pp. 14349-14358.  
 Kleinfeld, O., Frenkel A., Bogin, O., Eisenstein, M., Brumfeld, V., Burstein, Y. and Sagi, I. (2000), *Biochemistry*, **26**, pp. 7702-7711.  
 Korkhin, Y., Kalb, A.J., Peretz, M., Bogin, O., Burstein, Y., Frolow, F. (1998), *J. of Mol. Biol.*, **278**, pp. 967-981.  
 Peretz, M., Bogin, O., Keinan, E. and Burstein, Y. (1993), *Int. J. Pept. Protein Res.*, **42**, pp. 490-595.  
 Peretz, M., Weiner, L.M. and Burstein, Y. (1997), *Protein Sci*, **6**, pp. 1074-1083.  
 Rehr, J.J., Mustre, de leon, J., Zabinsky, S.I., Albers, R.C. (1991), *J. Amer. Chem. Soc.*, **113**, pp. 5135-5138.  
 Stern, E.A., Newville, M., Ravel, B., Yacoby, Y. and Haskel, D. (1995), *Physica B*, **208 & 209**, pp. 117-120.  
 Stoddared, B.L. (1996), *Nature Structure Biology*, **3**, pp. 907-909.  
 Wirt, M.D., Sagi, I., Chen, E., Frisbie, S, Chance, R.M. (1990), *J. Am. Chem. Soc.*, **113**, pp. 5299-5314.  
 Zabinsky, S.I., Rehr, J.J., Ankudinov, A., Albers, R.C. and Eller, M.J. (1995), *Phys. Rev. B*, **52**, pp. 2995-3009.